Branching ratios and bond dissociation energies from the excimer laser photolysis of group 6 metal carbonyls

D. M. Rayner, Y. Ishikawa, C. E. Brown, and P. A. Hackett

Citation: The Journal of Chemical Physics **94**, 5471 (1991); doi: 10.1063/1.460482
View online: http://dx.doi.org/10.1063/1.460482
View Table of Contents: http://scitation.aip.org/content/aip/journal/jcp/94/8?ver=pdfcov
Published by the AIP Publishing

Branching ratios and bond dissociation energies from the excimer laser photolysis of group 6 metal carbonyls[a)]

D. M. Rayner, Y. Ishikawa,[b)] C. E. Brown,[c)] and P. A. Hackett
Steacie Institute for Molecular Science, National Research Council Canada, 100 Sussex Drive, Ottawa, Ontario K1A 0R6, Canada

(Received 7 November 1990; accepted 9 January 1991)

Photolysis of the group 6 (Cr, Mo, W) metal carbonyls in the gas phase, at excimer laser wavelengths, may lead to more than one primary product. Branching ratios between these products have been measured as a function of photolysis wavelength, buffer gas pressure, and temperature using time-resolved infrared spectroscopy. The results are modeled using a sequential dissociation mechanism in which branching ratios are determined by competition between unimolecular dissociation and collisional relaxation. The sensitivity of the results to thermochemical input parameters and assumptions concerning energy disposal mechanisms is discussed. Under qualified assumptions the branching ratio measurements provide estimates for CO bond dissociation energies for coordinatively unsaturated metal carbonyls. For Mo and W the individual bond dissociation energies are close to the average values but for Cr the first three ligands coordinated are significantly less strongly bound than the last three. This finding is discussed in terms of recent *ab initio* calculations on bonding in metal carbonyls.

I. INTRODUCTION

It is now well established that the single-photon ultraviolet photolysis of transition metal carbonyls, $M(CO)_n$, in the gas phase can lead to photofragmentation extending beyond the loss of a single CO ligand. This is based on evidence from chemical trapping studies on $Fe(CO)_5$ (Ref. 1) followed, more recently, by a series of time-resolved infrared spectroscopic (TRIS) studies on $Fe(CO)_5$ (Ref. 2), $Cr(CO)_6$ (Refs. 3–5), $Mo(CO)_6$ (Refs. 5 and 6), $W(CO)_6$ (Refs. 5, 7), $V(CO)_6$ (Ref. 8), $Mn_2(CO)_{10}$ (Ref. 9), $Co(CO)_3NO$ (Ref. 10), $Ru(CO)_5$ (Ref. 11), and $Os(CO)_5$ (Ref. 12). These TRIS studies also showed that the extent of fragmentation increased with photon energy and that the nascent coordinatively unsaturated fragments ($M(CO)_x$) were produced with appreciable amounts of internal energy. It is generally accepted that these results indicate a sequential, CO elimination mechanism. At ultraviolet wavelengths the photon energy is significantly greater than the M—CO bond dissociation energy. Initial CO loss leaves a large portion of the excess energy in the nascent unsaturated fragment that then undergoes a series of spontaneous unimolecular CO eliminations, until the retained energy is insufficient to drive the sequence further, viz.

$$M(CO)_n + h\nu \rightarrow M(CO)_{n-1}^* + CO, \quad (1a)$$

$$M(CO)_{n-1}^* \rightarrow M(CO)_{n-2}^* + CO, \quad (1b)$$

$$M(CO)_{n-1}^* + X \rightarrow M(CO)_{n-1} + X, \quad (1c)$$

$$\vdots$$

$$M(CO)_{x+1}^* \rightarrow M(CO)_x^\dagger + CO, \quad (1d)$$

$$M(CO)_{x+1}^* + X \rightarrow M(CO)_{x+1} + X, \quad (1e)$$

$$M(CO)_x^\dagger + X \rightarrow M(CO)_x + X, \quad (1f)$$

where $M(CO)_x^*$ and $M(CO)_x^\dagger$ indicate $M(CO)_x$ internally excited above and below its dissociation limit, respectively, and X is the buffer gas. In solution, photolysis results in the loss of only one CO ligand regardless of the energy of the photolysis photons.[13] In this case rapid relaxation of $M(CO)_{n-1}^*$ to the solvent effectively halts the sequential reaction and the quantum yield is determined by the dynamics of interactions with the solvent cage.

A consequence of this sequential mechanism is that the photofragment distributions could show a dependence on the buffer gas pressure in addition to their dependence on the photolysis wavelength. Initially, relaxation to the buffer gas cannot compete with the unimolecular dissociation rate, but towards the end of the sequence such a competition may occur. Recently we reported the first observation of such a buffer gas pressure dependence in the 308 nm photolysis of $Cr(CO)_6$ in Ar.[5] The ratio of yields, $[Cr(CO)_4]/[Cr(CO)_5]$, measured using TRIS, was found to depend on Ar pressure, $p(Ar)$, in the range 2 to 100 Torr in a manner that could be modeled using unimolecular reaction theory. The model was found to be sensitive to a number of variables including: the bond dissociation energies $D[Cr(CO)_5—CO]$ and $D[Cr(CO)_4—CO]$; $\log A_\infty$ for the unimolecular dissociation of $Cr(CO)_5$; and, the models used to describe both energy partitioning in the initial photolyis of $Cr(CO)_6$ and collisional energy transfer.

Thermochemical information on organometallic compounds is relatively scarce, especially data that can be related to individual bonds in both stable and coordinatively unsaturated species. Average bond dissociation energies, D[M—CO], have been derived from calorimetric measurements of enthalpies of disruption.[14] However, recent work suggests that D[M—CO] is a poor approximation for the individual bond dissociation energies. Infrared laser sensitized pyrolysis has been used to estimate the first bond dissociation energies for $Fe(CO)_5$, $Cr(CO)_6$, $Mo(CO)_6$, and $W(CO)_6$. It is found that $D[M(CO)_{n-1}—CO]$ is signifi-

[a)] Issued as NRCC #32323.
[b)] NRCC Research Associate 1986–1988. Present address: Kyoto Institute of Technology, Matsugaski, Sakyoku, Kyoto 606, Japan.
[c)] NRCC Research Associate 1987–present.

cantly greater than $D[M—CO]$.[15] Electron detachment measurements for $Fe(CO)_5$[16] and $Ni(CO)_4$[17] suggest large variations in $D[M(CO)_x—CO]$ with x, although the error associated with these measurements may be large.[18] Unimolecular reaction theory has been applied to the recombination reactions of $Cr(CO)_5$ and $Cr(CO)_4$ with CO, monitored by TRIS, to obtain estimates for $D[Cr(CO)_5—CO]$ and $D[Cr(CO)_4—CO]$.[19] However, there is controversy in the literature over the rate of recombination of CO with group 6 tetracarbonyls[3-6] and these results too are in some doubt.

It is therefore of interest to investigate branching ratios in metal carbonyl photodissociation as they may provide information on individual bond energies. In addition, questions of photodissociation dynamics and energy disposal are also addressed by these experiments. In this paper we present details of the model we have used to fit branching ratios in the photodissociation of $Cr(CO)_6$ (Ref. 5) and discuss the sensitivity of the model to thermochemical input parameters and details of the dynamics of the photodissociation. The model is tested against our previous TRIS results on the 308 nm photolysis of $Cr(CO)_6$, against new results on the temperature dependance of this reaction, and against the pressure dependence of branching ratios observed in the excimer laser photolysis of other group 6 metal carbonyls. Interestingly the results show that for the second and third transition series elements individual metal ligand bond dissociation energies are much closer to the average value than for the first series element. In particular, for chromium hexacarbonyl, the average bond dissociation energy for the first three carbonyl ligands coordinated to chromium is approximately half that of the average bond dissociation energy for the last three ligands coordinated. We attribute this result to the importance of s—d promotion energies for the first transition series.

II. EXPERIMENTAL

Our time-resolved infrared spectrometer has been described in detail elsewhere.[7,8,10] Briefly, gas mixtures consisting of the metal hexacarbonyl ($\sim$5 mTorr) and Ar buffer gas (2–100 Torr) were flowed slowly through the brass reaction cell that had an effective path length of 12 cm for UV photolysis light and 24 cm for IR monitoring light. The temperature in the cell and in the stainless-steel gas delivery lines could be controlled in the range 25–90 °C. Gas temperatures were measured with a low heat capacity thermocouple placed just outside the reaction zone. The flowing sample was irradiated with an excimer laser (Lumonics 860-1 for XeF and KrF; 861-4 for XeCl and KrCl). The laser pulse width was $\sim$20 ns and a fluence of a few mJ cm^{-2} was typically employed. A line-tuneable, liquid-nitrogen-cooled, cw CO laser was used to detect transient intermediates in IR absorption by means of a MCT detector/fast preamplifier combination (rise time $\sim$300 ns). The preamplifier signal was fed to a Tektronix differential amplifier and a Biomation 8100 transient digitizer. The average of 100 traces was stored in a computer (DEC LSI 11/23). Time-resolved difference IR absorption spectra were reconstructed by the computer from transient absorption signals for each CO laser line. Relative yields of $M(CO)_x$ were obtained from transient absorption measurements at specific wavelengths identified from infrared assignments for CO stretching frequencies made in preceding work in these and other laboratories.[2-7] Advantage was taken of photolysis conditions that do not result in significant branching to establish the relative absorption coefficients required to convert absorption measurements to yields.

$Mo(CO)_6$, $Cr(CO)_6$, $W(CO)_6$, and $Fe(CO)_5$ were purchased from Alfa Products. They were degassed by several freeze-thaw cycles using dry ice/methanol and were used without further purification. Argon was obtained from Air Products (research grade, $>$99.995% purity).

III. MODEL

Our model, demonstrated here through its application to the 308 nm dissociation of $Cr(CO)_6$,

$$Cr(CO)_6 + h\nu \rightarrow Cr(CO)_6{}^{**}, \tag{2a}$$

$$Cr(CO)_6{}^{**} \rightarrow Cr(CO)_5{}^{*}, \tag{2b}$$

$$Cr(CO)_5{}^{*} + X \rightarrow Cr(CO)_5, \tag{2c}$$

$$Cr(CO)_5{}^{*} \rightarrow Cr(CO)_4, \tag{2d}$$

is similar in many aspects to descriptions of chemical and photoactivated unimolecular reactions.[20] $Cr(CO)_6$ starts in a thermal Boltzmann distribution,

$$P(E) = N(E)\exp(-E/kT)/Q, \tag{3}$$

where $N(E)$ is the density of states at an energy E referenced to the zero-point energy of $Cr(CO)_6$ and Q is the partition function for the internal modes of the molecule. Following absorption of an ultraviolet photon a linear transformation of this distribution describes the distribution of energy in the photoexcited molecules $Cr(CO)_6{}^{**}$,

$$\begin{aligned} &P(E) = N(E + D_6 - E_\lambda) \\ &\qquad \times \exp[-(E + D_6 - E_\lambda)/kT]/Q, \\ &E > (E_\lambda - D_6), \\ &P(E) = 0, \quad E \leqslant (E_\lambda - D_6), \end{aligned} \tag{4}$$

where E is now referenced to the zero-point energy of $Cr(CO)_5$, D_6 is $D[Cr(CO)_5 - CO]$, and E_λ is the photon energy. This distribution and details of the dynamics of the photodissociation determine the nascent distribution of energy in $Cr(CO)_5{}^{*}$, $F(E)$; for the moment we assume that this process is too rapid to be affected by collisions and that $Cr(CO)_5{}^{*}$ is in its ground electronic state. $Cr(CO)_5{}^{*}$ is lost through unimolecular reaction and through collisional relaxation with the bath gas, X. Competition between these processes is energy dependent, primarily through the energy dependence of the microscopic rate constant for dissociation, $k(E)$, which can be calculated through RRKM theory. In the strong collision limit the yields in the dissociation channel, ϕ_D, and the stabilization channel, ϕ_S are given by

$$\begin{aligned} &\phi_D = \int_{D_5}^{\infty} \frac{F(E)k(E)}{k(E)+\omega}\,dE, \quad \phi_S = \int_0^{\infty} \frac{F(E)\omega}{k(E)+\omega}\,dE, \\ &\phi_S + \phi_D = 1, \end{aligned} \tag{5}$$

where D_5 is $D[Cr(CO)_4 - CO]$ and ω is the collision fre-

quency. To allow for weak collisions, we have used a more complete description, which involves a multilevel description of the system, where the time dependence of the population of the ith energy level, n_i, is given by the master equation,

$$\frac{dn_i}{dt} = -k_i n_i - \omega n_i \sum_i q_{j\leftarrow i} + \omega \sum_j q_{i\leftarrow j} n_j, \tag{6}$$

where $q_{x\leftarrow y}$ are the transition probabilities and k_i is the rate constant for unimolecular reaction from the ith level. Here, ϕ_D and ϕ_S can be derived by numerical integration of this equation if $q_{x\leftarrow y}$ are known.

A. Energy disposal in the initial fragmentation step

Energy disposal in the photodecomposition of metal carbonyls has been the subject of three recent studies that determined either the disposal of energy in vibrational, rotational, and translational degrees of freedom of the CO fragment, $CO(v,J,E_T)$ or translational energy distributions in the metal carbonyl fragments. Waller and Hepburn[21] used VUV LIF to monitor CO produced in the collision-free ultraviolet photolysis (193, 248, 266, and 351 nm) of $Fe(CO)_5$ in a supersonic beam and found $CO(v,J,E_T)$ distributions in accordance with a statistical energy disposal model. Holland and Rosenfeld[22] used diode laser TRIS to monitor $CO(v,J,E_T)$ distributions following 351 nm photolysis of $W(CO)_6$, where only a single CO ligand is lost. Their results were tested against limiting case physical models including full and modified statistical theories. A modified statistical model fitted the vibrational distribution but their results were not conclusive regarding translational and rotational degrees of freedom. Venkataraman *et al.* have used molecular beam photofragment spectroscopy to estimate translational energy distributions in the 248 nm photolysis of $M(CO)_6$ (M = Cr, Mo, W).[23] Their findings are consistent with a model where translational energy from the primary photodissociation step is determined by a repulsive interaction whereas in subsequent steps it is determined by statistics.

We have tested several models in fitting our branching ratio measurements. As model I, we have reframed the statistical model, where equal probability is given to all product quantum states allowed by energy conservation, to predict the distribution of internal energy retained in the polyatomic metal carbonyl fragment. We follow the approach taken by Bogan and Setser[24] to predict prior distributions for energy disposal to HF in the abstraction of H atoms from polyatomic molecules by F atoms. In a unimolecular dissociation reaction the probability of observing a given internal energy, E_I, in a fragment, at a total fixed energy, E, is given by

$$G(E_I,E) = \frac{N(E_I,E)}{\sum_{E_I=0}^{E} N(E_I,E)}, \tag{7}$$

where $N(E_I,E)$ is the density of states for products with total energy E and E_I in the fragment. With the translational density of states proportional to $E_T^{1/2}$ (Ref. 25) and the rotational density of states of the polyatomic fragment proportional to $E_R^{1/2}$, in the classical limit, $N(E_I,E)$ is given by

$$N(E_I,E) \propto N_I(E_I) \sum_{v=0}^{v_{\max}} \sum_{J=0}^{J_{\max}} (2J+1) \times \int_0^{(E-E_I-E_v-E_J)} E_R^{1/2} \times (E-E_I-E_v-E_J-E_R)^{1/2}\, dE_R, \tag{8}$$

where $N_I(E_I)$ is the density of vibrational states for the polyatomic fragment, v and J are vibrational and rotational quantum numbers for the diatomic fragment, $E_v = vh\nu_{CO}$, and $E_J = B_{CO}\, J(J+1)$. Here, $v_{\max}$ and $J_{\max}$ are the maximum values of v and J allowed under the requirements that $E_v \leqslant E - E_I$ and $E_J \leqslant E - E_I - E_v$. Evaluation of the integral over E_R and the sum over J[26] leads to

$$G(E_I,E) = \frac{N_I(E_I)\sum_v^{v_{\max}}\{(E-E_I-E_v)^3 + (E-E_I-E_v)^2\}}{\sum_{E_I=0}^{E} N_I(E_I)\sum_v^{v_{\max}}\{(E-E_I-E_v)^3 + (E-E_I-E_v)^2\}}. \tag{9}$$

The above expression ignores angular momentum constraints. The second model, model II, attempts to take these into consideration to first order. Conservation of angular momentum requires that

$$\mathbf{J}_{\mathrm{REACT}} = \mathbf{J}_{\mathrm{FRAG}} + \mathbf{J}_{\mathrm{CO}} + \mathbf{L}, \tag{10}$$

where $\mathbf{J}_{\mathrm{REACT}}$, $\mathbf{J}_{\mathrm{FRAG}}$, $\mathbf{J}_{\mathrm{CO}}$ refer to the rotational angular momentum in the reactant and products and $\mathbf{L}$ is the product orbital momentum. For a symmetric top this leads to the requirement that

$$(J_{\mathrm{REACT}} - J_{\mathrm{CO}} - L) < J_{\mathrm{FRAG}} < (J_{\mathrm{REACT}} + J_{\mathrm{CO}} + L). \tag{11}$$

A consequence of the relative sizes of the reactant and the CO fragment and impact parameter considerations[22] is that the average value for J_{REACT},

$$\langle J_{\mathrm{REACT}} \rangle \gg J_{\mathrm{CO}} + L \tag{12}$$

for reactant molecules starting at a room temperature Boltzmann distribution. This implies that there are no significant angular momentum conservation restraints on partitioning to the CO fragment. However, as

$$J_{\mathrm{FRAG}} \simeq J_{\mathrm{REACT}}, \tag{13}$$

two of the rotational modes of the reactant are largely inactive in the dissociation. In this case $G(E_I,E)$ is given by

$$G(E_I,E) = \frac{N_I(E_I)\sum_v^{v_{\max}}(E-E_I-E_v)^2}{\sum_{E_I=0}^{E} N_I(E_I)\sum_v^{v_{\max}}(E-E_I-E_v)^2}. \tag{14}$$

A third model, model III, has all available energy retained as internal energy in the fragment except for that pre-

dicted by unimolecular reaction theory to partition to translational energy when CO is treated as a quasiatomic species. This approach is equivalent to the "statistical" model Yardley *et al.* applied to the photodissociation of $Fe(CO)_5$. The predicted product energy distribution is then[20b]

$$G(E_I,E) = \frac{N^\dagger(E_I)}{\Sigma_{E_I=0}^{E} N^\dagger(E_I)}, \tag{15}$$

where $N^\dagger(E_I)$ is the density of states in the transition complex at an energy E_I.

The final model, model IV, is based on the mechanism proposed by Venkataraman *et al.* for the 248 nm photolysis of $M(CO)_6$. They found empirically that their observed $M(CO)_x$ fragment translational energy distributions could be reproduced if the nascent distribution in $M(CO)_5$* had the form

$$G(E_I,E) = e^{-\beta(E-E_I-E_0)^2}, \tag{16}$$

where β and E_0 are fitted parameters.

Whichever form of $G(E_I,E)$ is used, the nascent distribution of energy in $Cr(CO)_5$* is given by the convolution

$$F(E) = \int_E^\infty P(E')G(E'-E,E')dE'. \tag{17}$$

B. Collisional deactivation

$F(E)$ sets the initial conditions for solution of the stabilization and deactivation yields under weak collision conditions [Eq. (6)]. We have employed the step ladder model that has been used extensively for chemical activation systems to model collisional transition probabilities through the region of reactive states.[20] In the present situation, the large internal energy allows up-transitions to be neglected. Down-transitions are taken to have a probability of 1 for the transfer of a fixed energy, set to the average energy transferred per collision, $\langle\Delta E\rangle$, and 0 for all other transitions. The total yield in the stabilization channel is then given by

$$\phi_s = \int_0^\infty F(E) \prod_i^0 \frac{\omega}{k(i\langle\Delta E\rangle)+\omega} dE,$$
$$= 1 - \phi_D. \tag{18}$$

C. RRKM calculations

The microscopic rate constant for dissociation of $Cr(CO)_5$* at an excess energy of E, $k(E)$ is given in RRKM theory by

$$k(E) = LW^\dagger(E-E_0)/hN(E), \tag{19}$$

where L is the reaction path degeneracy, $W^\dagger(E-E_0)$ is the sum of states in the transition state up to an internal energy $(E-E_0)$, $N(E)$ is the density of states in the reactant with energy, and E and E_0 is the critical energy for the reaction.[20] In a bond fission reaction E_0 is the bond dissociation energy, D_5 in this case, less a small contribution from the centrifugal effect of the adiabatic rotation. The form of $k(E)$ is dependent on the model chosen for the transition state as it determines the frequencies used to estimate $W^\dagger(E-E_0)$. Hence uncertainty about the transition state always qualifies calculation of $k(E)$. However, for bond-fission reactions of polyatomics of the size considered here, $k(E)$ proves empirically to be determined by only two factors, E_0 and $\log A_\infty$, where A_∞ is the A factor for the dissociation calculated by statistical mechanics. The dependence of $k(E)$ on E is virtually independent of the details of the transition state as long as they result in the same value of $\log A_\infty$. Here, E_0 and $\log A_\infty$ therefore become variable inputs for the model, $\log A_\infty$ being adjusted by tuning the low vibrational and/or internal rotations assigned to the transition complex.

The relative yields measured in our experiment are therefore a function of: the photon energy, E_λ, the dissociation energy, D_6, and temperature, T, through $P(E)$; the dissociation energy, D_5, and the associated A factor, A_∞, through $k(E)$; and pressure, p, and to a small extent T through $\omega = Zp$, where Z is the collision number. By studying the effect of the experimentally variable parameters p and T on the yields we are able to test aspects of the model including its sensitivity to the molecular constants D_6, D_5, and A_∞ and the energy disposal models.

IV. RESULTS AND DISCUSSION

A. 308 nm photolysis of $Cr(CO)_6$

Figure 1 shows the dependence of the ratio of product yields $[Cr(CO)_4]/[Cr(CO)_5]$, $= R$, on buffer gas (Ar) pressure. The experimental results are from our previous paper where the effect of $p(Ar)$ on TRIS observed following the 308 nm photolysis of $Cr(CO)_6$ at room temperature was analyzed in terms of a branching between $Cr(CO)_5$ and $Cr(CO)_4$ production. The line fitting closely to the experimental points is a result predicted using the model described above with energy disposal described by the full statistical model, model I. Agreement at both ends of the pressure range is emphasized by plotting R against both $1/p(Ar)$ and $p(Ar)$. The best fit was achieved by adjusting D_5 to 32.9 kcal mol^{-1} while keeping other parameters at their current best estimates. In this case we took $D_6 = 37$ kcal mol^{-1} from the

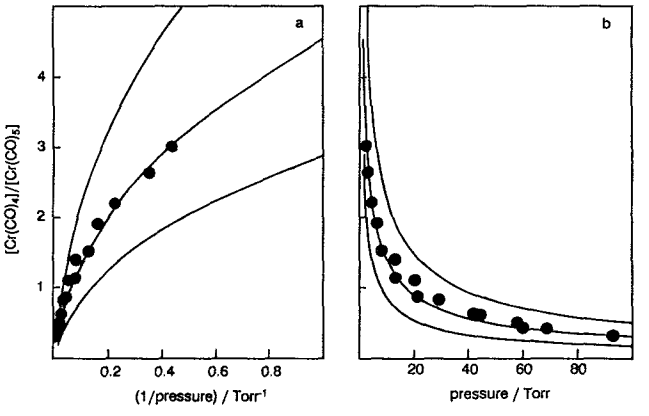

FIG. 1. The buffer gas (Ar) pressure dependence of the ratio of primary fragment yields, $[Cr(CO)_4]/[Cr(CO)_5]$, in the XeCl laser (308 nm, 3 mJ cm^{-1}) photolysis of $Cr(CO)_6$ ($\sim$10 mTorr) as measured by TRIS. The line through the points is a best fit through the points obtained using model I (see text) with $D_6 = 37$ kcal mol^{-1}, $\log A_\infty = 15.4$ and $D_5 = 32.9$ kcal mol^{-1}. The flanking lines are found with D_5 adjusted by ± 1 kcal mol^{-1}.

Bernstein *et al.* photoacoustic calorimetric value of 37 ± 5 kcal mol^{-1} (Ref. 27) and from Lewis *et al.*'s laser pyrometric value of 36.8 ± 3 kcal mol^{-1} (Ref. 15). We took $\log A_\infty = 15.4$. This is the value used by Lewis *et al.* in their analysis for D_6 and is reasonable in terms of measurements for other metal carbonyls ($Fe(CO)_5$, $\log A_\infty = 15.8$; $Mo(CO)_6$ and $W(CO)_6$, $\log A_\infty = 15.6$), other diatomic releasing bond dissociation reactions ($\log A_\infty = 15.6$ to 16.3), and the expectations of transition state theory.[15] Here, Z was estimated as 7.4×10^{-10} molecule^{-1} cm^3 s^{-1} (2.6×10^7 Torr^{-1} s^{-1}) from a collision diameter of 6.1 Å and $\langle\Delta E\rangle$ was set at 0.5 kcal mol^{-1}, which is of the order found for Ar relaxation of large organic polyatomic molecules at the excess energies relevant here.[28]

Our first conclusion is that the experimental results can be described very well by the full statistical version of the model proposed here. A second conclusion is that the fit is very sensitive to the variable parameter, in this case D_5. The flanking lines in Fig. 1 are plotted with D_5 adjusted by only 1 kcal mol^{-1} in either direction. If we were certain of the values of the other input parameters and the energy disposal mechanism our experiment would fix D_5 to within ± 0.2 kcal mol^{-1}. Unfortunately, as the following sensitivity analysis shows, this fit is by no means exclusive. Figure 2 shows that equally good fits can be obtained for other sets of input parameters. In Fig. 2(a) D_6 has been adjusted by -5 to 32 kcal mol^{-1} and the fit shown is found with $D_5 = 35.3$ kcal mol^{-1}. In Fig. 2(b) $\log A_\infty$ has been increased to 16.8 by adjusting the transition complex frequencies and the fit shown is found with $D_5 = 36.2$ kcal mol^{-1}. Figure 3 shows the surface of D_6, D_5, and $\log A_\infty$ values that result in acceptable fits to the data. The surface is a tipped plane, described by

$$D_5 = (11.8 - 0.47D_6 + 2.5 \log A_\infty)\text{kcal mol}^{-1},$$

and linear extrapolation can be used effectively to predict the third parameter if the other two are known.

The effects of changing $\langle\Delta E\rangle$ and Z are shown in Fig. 4. Acceptable fits are found for $\langle\Delta E\rangle$ in the range 1 to 0.2 kcal mol^{-1} and for collision frequencies in the range 1.3 to 5.2×10^7 Torr^{-1} s^{-1} but for large $\langle\Delta E\rangle$ and the limiting strong collision model the fits are unacceptable. Thus our results are sufficiently sensitive to the collisional deactivation mechanism to identify the requirement to describe the relaxation by a weak collision model but not sensitive enough to reveal details other than a range of acceptable collision parameters. From theoretical and experimental studies on collisional relaxation of large molecules we expect $\langle\Delta E\rangle$ to be a linear function of excess energy at the energies involved here.[28] However the bulk of branching occurs over a relatively narrow range of energies where $k(E)$ and ω compete effectively and over which $\langle\Delta E\rangle$ is essentially constant. We do not expect to learn anything further by refining the model to allow for the varition of $\langle\Delta E\rangle$ with E. From Fig. 4 we can conclude that uncertainty in $\langle\Delta E\rangle$ and Z shows up as an uncertainty in the D_6, D_5, $\log A_\infty$ surface of Fig. 3 of $\sim \pm 1$ kcal mol^{-1} in the D_5 coordinate.

A second experimentally accessible variable is temperature. In our model, temperature has its main result in chang-

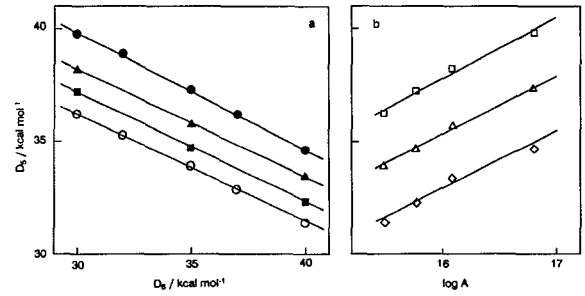

FIG. 3. The surface of D_6, D_5, and $\log A_\infty$ values that result in acceptable fits to the $[Cr(CO)_4]/[Cr(CO)_5]$ pressure dependence. (a) ○ $\log A_\infty = 15.4$, ■ $\log A_\infty = 15.8$, ▲ $\log A_\infty = 16.1$, ● $\log A_\infty = 16.8$. (b) ◇ $D_6 = 40$ kcal mol^{-1}, △ $D_6 = 35$ kcal mol^{-1}, □ $D_6 = 30$ kcal mol^{-1}.

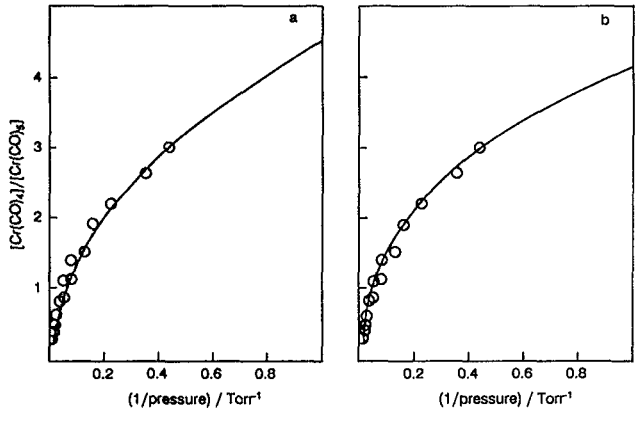

FIG. 2. Effect of varying the model input parameters, D_6 and $\log A_\infty$, on the quality of fit: (a) $D_6 = 32$ kcal mol^{-1}, lowered by 5 kcal mol^{-1} with respect to Fig. 1, fit found for $D_5 = 35.3$ kcal mol^{-1}; (b) $\log A_\infty = 16.8$, raised by 1.4 compared with that used in Fig. 1, fit found for $D_5 = 36.2$ kcal mol^{-1}.

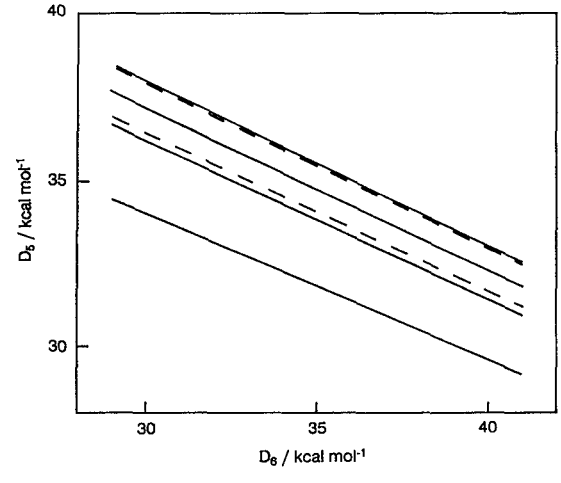

FIG. 4. Effect of collision parameters in modeling fragment branching ratios. The lines map the (D_6, D_5) combinations that produce best fits to the $[Cr(CO)_4]/[Cr(CO)_5]$ data for different values of $\langle E\rangle$ and Z. The solid lines are, in descending order for $\langle E\rangle = 0.2$, 0.5, 1, and 10 kcal mol^{-1} with $Z = 2.6\times10^7$ s^{-1} Torr^{-1}. For $\langle E\rangle = 10$ kcal mol^{-1} the fits become unacceptable. The dashed lines are, in descending order, for $Z = 1.3$ and 5.2×10^7 s^{-1} Torr^{-1} with $\langle E\rangle = 0.5$ kcal mol^{-1}.

ing $P(E)$. Its effect on Z is relatively minor. Figure 5 shows results obtained at 364 K contrasted with room temperature results. The curve through the high-temperature data was obtained by adjusting only the temperature in the model to 364 K, leaving all other parameters as found from the room temperature data. The resulting fit is as good as could be found by any arbitrary adjustment of the other input parameters and increases confidence in our model. Unfortunately the temperature results do not allow us to restrict the surface of acceptable input parameters. Similar agreement at two temperatures can be demonstrated for other sets of input parameters.

The effect of the energy disposal model is shown in Fig. 6. Models I and II both give acceptable fits but model III [Fig. 6(a)] does not. Like the collision parameters the choice of model has the effect of adjusting the level of the D_6, D_5, $\log A_\infty$ surface in the D_5 coordinate. Inclusion of angular momentum constraints in the energy disposal model (model II) raises D_5 by ~ 1 kcal mol^{-1}. Recognizing that the fits are no longer acceptable, model III, which treats the CO fragment as a quasiatom, raises D_5 by ~ 4 kcal mol^{-1}. If the disposal models are characterized by the fraction of excess energy retained in the fragment then the more energy that is retained, the higher D_5 is required to be. It is not however sufficient to describe the energy disposal simply by an average energy retained. If the same average energy found to be retained from model I is applied as a delta function rather than $G(E_I,E)$ calculated via Eq. (9) then the fit is very poor indeed [Fig. 6(b)]. Satisfactory fits can also be obtained using the empirical distributions of the type attributed to the repulsive first step model, model IV. However in the absence of a detailed model for the repulsive mechanism, including the effect of coupling into orthogonal vibrations and detailed knowledge of the dynamics of the different excited states populated by 308 rather than 248 nm excitation, we can have no prior expectations as to the magnitude of the β and E_0 parameters that might be applicable at 308 nm, if indeed repulsive dynamics operate at this wavelength. In the case of model III the poor fit can be attributed to the narrowness of $G(E_I,E)$ as calculated from Eq. (15). Empirically

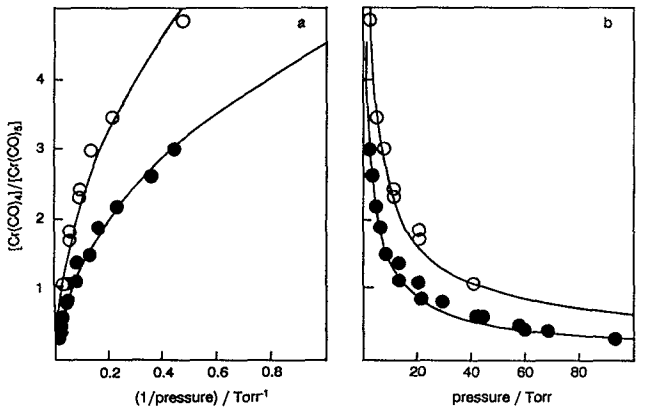

FIG. 5. Effect of temperature on $[Cr(CO)_4]/[Cr(CO)_5]$ in the 308 nm photolysis of $Cr(CO)_6$; ● 297 K, ○ 364 K. The fits shown are found using model I for identical input parameters except temperature that was set at the measured value.

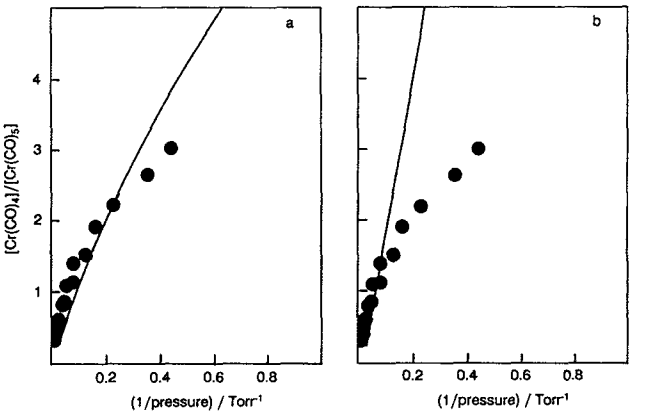

FIG. 6. Effect of the model chosen to describe energy disposal in the initial fragmentation step in modeling fragment branching ratios. (a) model III (in which the CO fragment is treated as a quasiatom, see text), (b) delta function model (see text).

our results require that, whatever the photodissociation dynamics of $Cr(CO)_6$ are, they must result in a relatively broad distribution of energies in nascent $Cr(CO)_5$*. Unlike chemical activation and direct photoactivation systems, where $F(E)$ is relatively narrow and "turn-up" in D/S plots is a consequence of multistep collisional deactivation, the curvature in our results is demonstrably due to a wide distribution in $F(E)$ that must be introduced in the step which produces $Cr(CO)_5$*. Such broadening is reasonably expected from dynamics which result in statistical energy distribution over a large number of accessible states. Both models I and II fit this bill. In the statistical model the states of the diatomic play a significant role in broadening $F(E)$ and making it peak at nonzero E. The Yardley *et al.* conclusion that $Fe(CO)_5$ photodissociation was nonstatistical[1] may well be due to their approximation of CO as an atom in their simplified "statistical" model. If the first step has a repulsive element at 308 nm then significant coupling to vibrational modes must be operative to broaden $G(E_I,E)$ and partition most of the excess energy to the internal modes of $Cr(CO)_5$*.

In the general application of the model to $M(CO)_6$ photodissociation we expect to observe pressure and temperature dependences of relative yields whenever branching in primary products has been observed. Branching has been observed in: the 222 nm photolysis of $Cr(CO)_6$ [$Cr(CO)_4/Cr(CO)_3$]; the 351 nm photolysis of $Mo(CO)_6$ [$Mo(CO)_5/Mo(CO)_4$);] and the 248 nm photolysis of $Mo(CO)_6$ [$Mo(CO)_4/Mo(CO)_3$].[5]

B. 351 nm photolysis of $Mo(CO)_6$

In this case the two primary products observed are $Mo(CO)_5$ and $Mo(CO)_4$ and the models developed for $Cr(CO)_6$ photolysis at 308 nm can be applied without further modification. Unfortunately, we were not able to obtain good data on the branching ratio over a large enough pressure range, due to experimental difficulties caused by the low vapor pressure of $Mo(CO)_6$ and its low absorption coefficient at 351 nm. We were able to observe a temperature

dependence of $[Mo(CO)_4]/[Mo(CO)_5]$ at $p(Ar) = 6$ Torr. The ratio of transient absorbance at 1975 cm^{-1} to that at 1989 cm^{-1}, OD_{1975}/OD_{1989} is ~ 0.8 at 298 K and ~ 1.6 at 363 K. From an estimate of relative extinction coefficients made from TRIS taken following the 308 nm photolysis of $Mo(CO)_6$ in the presence of CO[5] this implies $[Mo(CO)_4]/[Mo(CO)_5] = 0.4$ at 298 K and 0.8 at 363 K. Taking $D_6 = 40$ kcal mol^{-1} from the laser photolysis study of Lewis *et al.*,[15] $\log A_\infty = 15.8$ and model I for energy disposal, we find that setting $D_5 = 29.5$ kcal mol^{-1} predicts the ratios observed at both temperatures. Empirically the surface which reproduces the experimental results is given by

$$D_5 = (16.34 - 0.54D_6 + 2.2 \log A_\infty) \text{ kcal mol}^{-1}$$

in the ranges $D_6 = 35$ to 45 kcal mol^{-1} and $\log A_\infty = 15.4$ to 16.8. As for $Cr(CO)_6$, using model II to describe energy disposal will raise D_5 by ~ 1 kcal mol^{-1}. Uncertainties in D_5 introduced by collision parameters also prove to be of the same degree as for $Cr(CO)_6$, i.e. ± 1 kcal mol^{-1}.

C. Branching between $M(CO)_4$ and $M(CO)_3$

In the case of $Mo(CO)_6$ photolysis at 248 nm and $Cr(CO)_6$ photolysis at 222 nm, branching between $M(CO)_4$ and $M(CO)_3$ is observed. Modeling these results requires an extension of the model used for systems where branching is between $M(CO)_5$ and $M(CO)_4$. The nascent energy distribution in $M(CO)_5$* is calculated as before. Generally one would then compute the energy distribution of dissociating molecules and carry the reaction to the next step. In the two cases considered here we found that the photolysis energies are high enough that effectively all the $M(CO)_5$* are at energies where they dissociate before collisional activation can occur and that the distribution in dissociating $M(CO)_5$* is the same as the nascent distribution. The distribution in dissociating $M(CO)_5$* can then be used, in place of the shifted thermal initial distribution used for $M(CO)_6$, as $P(E)$ to calculate the nascent distribution in $M(CO)_4$*.

Figure 7 shows the effect of pressure and temperature on the ratio, $[Mo(CO)_3]/[Mo(CO)_4]$, observed in the 248 nm photolysis of $Mo(CO)_6$. In this case the ratio was calculated from the transient absorbances at 1969 cm^{-1} $[Mo(CO)_4]$ and 1891 cm^{-1} $[Mo(CO)_3]$. From $M(CO)_6$ TRIS at 308 and 222 nm (Ref. 5) we have established that there is no spectral overlap at these frequencies and have estimated the ratio of extinction coefficients as 1.0 ± 0.5. The fits shown in the figure are found for $D_6 = 40$ kcal mol^{-1}, $D_5 = 29.5$ kcal mol^{-1}, $\log A_\infty = 15.8$, and D_4 adjusted to 31 kcal mol^{-1} using the full statistical model. The fits are reasonable and are not improved by adjusting D_6 or D_5. Again the observed temperature behavior can be accounted for simply by adjusting the temperature in the model. If D_6, D_5, and $\log A_\infty$ are allowed to take extreme values on the surface which fitted our results for the 351 nm photolysis of $Mo(CO)_6$, D_4 is restricted to the range 30–32 kcal mol^{-1}. Figure 8 shows a similar treatment of the results for the 222 nm photolysis of $Cr(CO)_6$. The fits shown are found

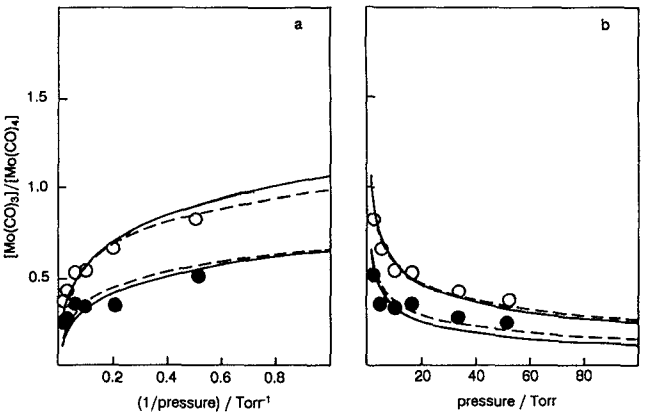

FIG. 7. The buffer gas (Ar) pressure dependence of the ratio of primary fragment yields, $[Mo(CO)_3]/[Mo(CO)_4]$, in the KrF laser (248 nm, 3 mJ cm^{-1}) photolysis of $Mo(CO)_6$ (~ 12 mTorr), as measured by TRIS, at 297 K, ●, and 362 K, ○. The solid lines through the points are obtained using model I, the dashed lines using model IV.

for $D_6 = 37$ kcal mol^{-1}, $D_5 = 33$ kcal mol^{-1}, $\log A_\infty [Cr(CO)_5 \rightarrow Cr(CO)_4] = 15.8$ and D_4 adjusted to 39 kcal mol^{-1}.

At this degree of dissociation our model qualitatively reproduces the temperature and pressure dependence of the branching, however in detail the fits are not as good. This is not surprising. Systematic effects of assumptions in the model will multiply as a function of the number of steps considered. In addition the experimental error is higher for these results. It is harder to estimate relative extinction coefficients reliably and there is the added complication of underlying absorption due to hot CO in experiments which employ higher photon energies. The excess energy for the first step in the 222 nm photolysis of $Cr(CO)_6$ is 92 kcal mol^{-1}. If the discrepancy between the model and experimental results has any significance then the suggestion is that either the distribution in $M(CO)_4$* is not calculated to be broad enough by our model or that $k(E)$ as calculated by RRKM theory does not rise steeply enough to allow a significant

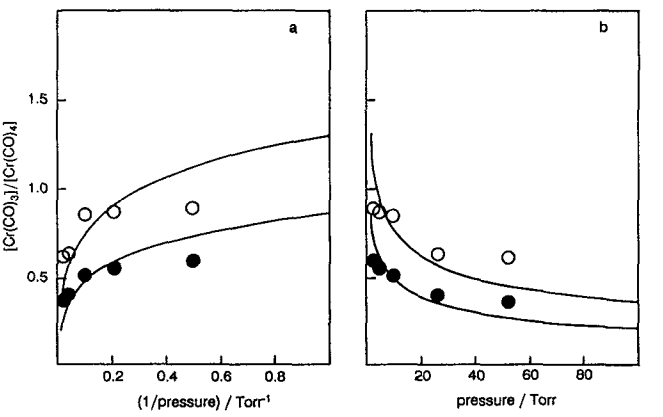

FIG. 8. The buffer gas (Ar) pressure dependence of the ratio of primary fragment yields, $[Cr(CO)_3]/[Cr(CO)_4]$, in the KrCl laser (222 nm, 5 mJ cm^{-1}) photolysis of $Cr(CO)_6$ (~ 6 mTorr), as measured by TRIS, at 297 K, ●, and 362 K, ○. The lines through the points are obtained using model I.

proportion of $M(CO)_4$* to be stabilized even at low pressures. Here, $k(E)$ rises more steeply the greater $\log A_\infty$ and we found that the model fitted the data better in these cases with $\log A_\infty = 16.8$, the highest value considered. Confidence in the experimental ratios at the shorter wavelengths is not sufficient to allow the assertion that $\log A_\infty$ is greater for the dissociation of the smaller fragments, indeed it is perhaps more reasonable to assume that the initial photodissociation is more repulsive at higher photon energies.

For $Mo(CO)_6$ photolysis at 248 nm we have the opportunity to compare our results directly with those of Venkataraman *et al.* Using their reported values for β and E_0 in the repusive first step model, model IV, we obtain the fits shown in Fig. 7. These fits, including the fit at the higher temperature that was found again by adjusting only T, are as acceptable as those found by the full statistical model and to this extent there is agreement between our yield results and their translational energy distribution measurements. Using this model, with $D_6 = 40$ kcal mol^{-1}, $D_5 = 29.5$, and $\log A_\infty = 15.8$ from our 351 nm result, we find $D_4 = 31$ kcal mol^{-1}, the same result as obtained from the full statistical model. Once again the branching ratio measurements are sensitive to the detailed dynamics of the photodissociation. Both the full statistical and the phenomenological repulsive models predict $M(CO)_5$* energy distributions which are consistent with the yield measurements. In the first case the required width in the distribution results from prior expectations of the model. In the second case the width of the distribution arises directly from the measured translational energy distributions assuming that the remaining excess energy is partitioned among the vibrational modes of the fragment metal carbonyl.

D. $W(CO)_6$ photolysis

For $W(CO)_6$, $W(CO)_5$ is the only fragment observed at 351 nm and 308 nm and $W(CO)_4$ is the only fragment observed at 248 and 222 nm (Refs. 5 and 7). If the as yet unobserved $W(CO)_3$ molecule has similar infrared absorption properties to $Cr(CO)_3$ and $Mo(CO)_3$ and making the conservative assessment that the TRIS experiment will detect any fragment that accounts for $> 20\%$ of the total fragment concentration, i.e., branching will be observed at least for $R = 5$ to 0.2, then, taking $D_6 = 46$ kcal mol^{-1} (Ref. 15), $\log A_\infty = 15.8$, and using model I, we find that D_5 must be in the range 36–39 kcal mol^{-1}, with the lower bound set by the absence of absorption attributable to $W(CO)_4$ in the 308 nm photolysis and the upper bound by the absence of $W(CO)_5$ in the 248 nm photolysis. In turn with $D_5 = 38$ kcal mol^{-1} the absence of $W(CO)_3$ in detectable quantities implies that $D_4 > 33$ kcal mol^{-1}.

E. Bond dissociation energies

Results for M—CO bond dissociation energies are summarized in Table I. The errors on the values we have estimated for D_5 and D_4 have been discussed above and to a degree they are dependent upon the value we have used for D_6. As discussed above, D_6 was assumed to be given by the value obtained in the homogeneous pyrolysis study of Lewis *et al.*[15] Nonetheless, the values reported in Table I are interesting in this respect: The values and trends in individual bond dissociation energies D_6, D_5, and D_4 do not correlate with the strong trend in the average bond dissociation energy observed in passing down the group. D_{av} is 26 kcal mol^{-1} for $Cr(CO)_6$, 36 kcal mol^{-1} for $Mo(CO)_6$, and 42 kcal mol^{-1} for $W(CO)_6$. This prompted us to compute $D_{\langle 6-4\rangle} = (D_6 + D_5 + D_4)/3$ and $D_{\langle 3-1\rangle} = (D_3 + D_2 + D_1)/3$. These parameters show some clear and interesting trends and are listed separately in Table II.

The results presented in Table II are interesting in this respect: for chromium $D_{\langle 6-4\rangle}/D_{\langle 3-1\rangle} \approx 2$ whereas for both molybdenum and tungsten $D_{\langle 6-4\rangle}/D_{\langle 3-1\rangle} \approx 1$. An implication of this result is that, for the 5th and 6th row elements, individual bond dissociation energies are close to the average value whereas, for the 4th row element the first ligands coordinated are less strongly bound than the last. A simplified factor behind this observation can be given. In order to bind six CO ligands the metal atom has to achieve a d^6 configuration. Our results imply that the energy cost for this promo-

TABLE I. M—CO bond dissociation energies, D_x/kcal mol^{-1}, in group 6 $M(CO)_x$ species.

					$\log A_\infty$	
	D_{av}	D_6	D_5	D_4	(5→4)	(4→3)
Cr	26[a]	37[b]	33[c]	39[c]	15.4	15.8
			25 ± 5[d]			
			40 ± 15[e]	20 ± 15[e]		
Mo	36[a]	40[b]	29.5[c]	31[c]	15.8	15.8
			35 ± 15[e]	30 ± 15[e]	15.8	15.8
W	42[a]	46	36–39[c]	> 33[c]	15.8	15.8
			40 ± 15[e]	25 ± 15[e]		

[a] Average bond dissociation energies from Ref. 14.
[b] Reference 18.
[c] This work, using D_6 and $\log A_\infty$ as given in the table and model I to describe energy disposal in the photodissociation. See text for confidence in these values.
[d] Reference 19.
[e] Reference 23.

TABLE II. Average M—CO dissociation energies, kcal mol^{-1}, for group 6 metal carbonyls.

	$D_{A\rangle}$	$D_{\langle 6-4\rangle}$	$D_{\langle 3-1\rangle}$
Cr	26	36	15
Mo	36	33	39
W	42.5	>38	<47

tion is paid later on in the coordination sequence as one goes down the group 6 column or, more likely, that this promotion energy is greater for chromium than for molybdenum and tungsten. The ground state configurations for chromium, molybdenum, and tungsten are $3d^5 4s^1$, $4d^5 5s^1$, and $5d^4 6s^2$, respectively. The promotion energy to the lowest lying d^6 configuration is 101 kcal mol^{-1} for chromium and 74 kcal mol^{-1} for molybdenum. This promotion energy is not known for tungsten.

It is more than simplistic to discuss as complex an issue as the dative bonding of carbonyl ligands to metal atoms from three different rows in the periodic table in terms of a single parameter. Individual ligand binding energies for Sc, Ti, and V mono- and dicarbonyls have been calculated by Barnes and Bauschlicher[29] using *ab initio* theory with very large Gaussian basis sets and extensive treatment of electron correlation. The strength of individual M—CO bonds is determined by several factors affecting the balance between π donation from the metal to carbon monoxide and the repulsion between σ electrons. In general terms, the repulsion, which is primarily caused by the metal's outer s electrons, can be reduced by either $s-p_\sigma$ or $s-d_\sigma$ hybridization and/or s to d promotion. These mechanisms are modified by the energy cost of reduced exchange interaction, and change as the number of ligands coordinated increases. As an example, Barnes and Bauschlicher find that the monocarbonyls of Sc, Ti, and V correlate with the $3d^n 4s^1$ asymptote that can reduce repulsion by polarizing the s electron away from CO maintaining a high spin state. For the dicarbonyls, however, the situation is not so clear. Intermediate and low spin states become more favored as they favor π donation. For dicarbonyls and presumably beyond, higher levels of calculation are required in order to reflect the subtleties of the bonding.

Few calculations have addressed the changes in bonding occurring down a group in the transition series. Such calculations are notoriously difficult, in part due to the increasing importance of relativistic effects and the difficulty in obtaining accurate and reliable basis sets. Barnes, Rosi, and Bauschlicher have recently published calculations on the first and second row transition metal mono- and dicarbonyl positive ions.[30] When referenced to common asymptotes there are no strong trends between the first and second transition series. However, it should be noted that the bonding here is somewhat simpler and may be explained in terms of a dominant electrostatic interaction. Interestingly, the calculated dissociation energies are in good accord with experiment except in the case of molybdenum. It will be interesting to see whether the more difficult calculations on the second transition series mono- and dicarbonyls will confirm the effect we report.

Further support for our observations can be obtained from studies of the photochemistry of group 8 pentacarbonyls. Although detailed branching ratio measurements have not been made on Fe, Ru, and Os, rough estimates can be made from the TRIS studies of Weitz and co-workers[2,11,12] using the models presented here. Like the group 6 carbonyls, D_{av} is much smaller for the fourth row element than the other two (D_{av} = 28, 41, and 45 kcal mol^{-1} for Fe, Ru, and Os, respectively[14]). The reported fragment distributions [351 nm photolysis of $Fe(CO)_5$—mainly $Fe(CO)_3$; 248 nm photolysis of $Fe(CO)_5$–$Fe(CO)_3 \approx Fe(CO)_2$; 248 nm photolysis of $Ru(CO)_5$—mainly $Ru(CO)_3$; 248 nm photolysis of $Os(CO)_5$—mainly $Os(CO)_3$] lead to the estimates that, for Fe, $D_{\langle 5-3\rangle}$, $\approx$34 kcal mol^{-1} and $D_{\langle 2-1\rangle} \approx 19$ kcal mol^{-1} while, for Ru, $D_{\langle 5-4\rangle} \approx 45$ and $D_{\langle 3-1\rangle} \approx 38$ kcal mol^{-1} and for Os $D_{\langle 5-4\rangle} \approx D_{\langle 3-1\rangle} \approx 45$ kcal mol^{-1}. As found for group 6 metal carbonyls, $D_{\langle 5-3\rangle}$ is significantly greater than $D_{\langle 2-1\rangle}$ for the 4th row element. Differences in the promotion energies to the lowest d^8 configuration (94 kcal mol^{-1} for Fe and 30 kcal mol^{-1} for Ru) are consistent with this observation.

Ab initio calculations on bonding in $Ni(CO)_x$ show that each CO ligand binds with approximately the same energy (30 kcal mol^{-1}).[31] As a result of the low-lying $^1D(3d^9 4s^1)$ and $^1S(3d^{10})$ configurations of nickel, all $Ni(CO)_x$ species, even the monocarbonyl, have low spin ground states. The invariance of D_x with x, which contrasts with behavior observed in the early first row elements,[29] is attributed to small promotion energies. For all group 6 metals we find D_6, D_5, and $D_4 \approx D_{\langle 6-4\rangle}$ which is consistent with the picture that the metal retains the same atomic configuration in $M(CO)_x$ for $x = 3$ to 6. This is in agreement with their geometric structures which can be rationalized on the basis of low spin complexes involving a d^6 metal centre.[32,33]

V. CONCLUSIONS

Fragment branching ratios clearly carry significant information on both the thermochemistry and photodissociation dynamics of metal carbonyls. It is premature to claim that individual CO bond dissociation energies can be determined unambiguously from these measurements through the modeling presented above. The models do show that the crucial molecular parameters, determining the branching and its pressure and temperature dependence, are the individual bond dissociation energies, the A factor associated with the branching step, and the dynamics that influence energy disposal down the sequence of dissociation steps. Collisional relaxation also plays an important role but is adequately described by a weak collision model with reasonable collision parameters. In respect to the dynamics the measured branching ratios require that the majority of the excess energy at each step is retained as internal excitation in the polyatomic fragment with a relatively broad distribution over vibrational states. This requirement is answered well by a full statistical model for each step where equal probability is given to all the product quantum states allowed by energy conservation. It can also be met by other models including both a refinement of the full statistical treatment that accounts for angular momentum conservation and an empiri-

cal treatment that allows for a degree of repulsive character in the primary photodissociation channel.

Major features of all the models investigated are a high sensitivity to the thermodynamic input parameters and a marked degree of correlation between them. Thus if all but one of the required bond energies and $\log A_\infty$ are known then the unknown parameter is established with reasonable precision (± 0.2 kcal mol^{-1}). Uncertainties in known CO bond dissociation energies make it difficult to take advantage of this. As our knowledge of metal carbonyl thermochemistry and photodissociation mechanisms improves, the results presented here will take greater meaning in terms of defining individual CO binding energies in coordinatively saturated and unsaturated metal carbonyls.

Although the individual bond dissociation energies reported here are subject to the uncertainties discussed above, trends in the binding for group 6 metal carbonyls are clear. In particular our results imply that, for Mo and W individual bond dissociation energies are close to the average values whereas for Cr the first ligands coordinated are less strongly bound than the last. This behavior appears to be repeated in the group 8 carbonyls. It can be rationalized in terms of a decreased importance, down the group, of the promotion energy required to reach the bonding configuration of the metal atom in order to coordinate the first one, two, or three ligands.

Note added in proof. Since this article went to press Barnes, Rosi and Bauschlicher have published results of an *ab initio* study of $Fe(CO)_n$, $n = 1,5$ [J. Chem. Phys. **94**, 2031 (1991)]. After scaling their energies to the experimental value for the enthalpy of disruption of $Fe(CO)_5$ one obtains $D_{\langle 5-3\rangle} = 41$ kcal mol^{-1} and $D_{\langle 2-1\rangle} = 10$ kcal mol^{-1}.

APPENDIX: COMPUTATIONAL ASPECTS

State counting, as required to calculate densities and sums of densities of states for evaluation of $P(E)$, $G(E)$ and $k(E)$, was carried out by direct count using the Beyer–Swinehart algorithm.[34,35] Frequencies for the unsaturated fragments were estimated from the parent frequencies which are available in the literature.[36]

To avoid the repeated counting to evaluate $G(E_l,E)$ from Eqs. (9), (14), and (15), case specific empirical analytical functions were sought that described $G(E_l,E)$ as calculated by state counting. Suitable expressions for the full and rotationally restricted statistical models have the form

$$G'(E_l,E) = (E - E_l)^a \exp\left[-\left(\frac{E - E_l}{cE + d}\right)^b \right], \qquad \text{(A1)}$$

where a, b, c, and d are constants.

[1] G. Nathanson, B. Gitlin, A. M. Rosan, and J. T. Yardley, J. Chem. Phys. **74**, 361 (1981); J. T. Yardley, B. Gitlin, G. Nathanson, and A. M. Rosan, *ibid.* **74**, 370 (1981).
[2] T. A. Seder, A. J. Ouderkirk, and E. Weitz, J. Chem. Phys. **85**, 1977 (1986).
[3] T. A. Seder, S. P. Church, and E. Weitz, J. Am. Chem. Soc. **108**, 4721 (1986).
[4] T. R. Fletcher and R. N. Rosenfeld, J. Am. Chem. Soc. **107**, 2203 (1985).
[5] Y. Ishikawa, C. E. Brown, P. A. Hackett, and D. M. Rayner, J. Phys. Chem. **94**, 2404 (1990)
[6] J. A. Ganske and R. N. Rosenfeld, J. Phys. Chem. **93**, 1959 (1989).
[7] Y. Ishikawa, P. A. Hackett, and D. M. Rayner, J. Phys. Chem. **92**, 3863 (1988).
[8] Y. Ishikawa, P. A. Hackett, and D. M. Rayner, J. Am. Chem. Soc. **109**, 6644 (1987).
[9] T. A. Seder, S. P. Church, and E. Weitz, J. Am. Chem. Soc. **108**, 7519 (1986).
[10] D. M. Rayner, A. S. Nazran, M. Drouin, and P. A. Hackett, J. Phys. Chem. **90**, 2882 (1986).
[11] P. L. Bogdan and E. Weitz, J. Am. Chem. Soc. **111**, 3163 (1989).
[12] P. L. Bogdan and E. Weitz, J. Am. Chem. Soc. **112**, 639 (1990).
[13] G. L. Geoffroy and M. S. Wrighton, *Organometallic Photochemistry* (Academic, New York, 1979).
[14] J. A. Connor, Topics Curr. Chem. **71**, 71 (1977).
[15] K. E. Lewis, D. M. Golden, and D. M. Smith, J. Am. Chem. Soc. **106**, 3905 (1986).
[16] P. C. Engleking and W. C. Lineberger, J. Am. Chem. Soc. **101**, 5569 (1979).
[17] A. E. Stevens, C. S. Feigerle, and W. C. Lineberger, J. Am. Chem. Soc. **104**, 5026 (1982).
[18] M. Poliakoff and E. Weitz, Acc. Chem. Res. **20**, 408 (1987).
[19] T. R. Fletcher and R. N. Rosenfeld, J. Am. Chem. Soc. **110**, 2097 (1988).
[20] (a) P. J. Robinson and K. A. Holbrook, *Unimolecular Reactions* (Wiley–Interscience, New York, 1972); (b) W. Forst, *Theory of Unimolecular Reactions* (Academic, New York, 1973).
[21] I. M. Waller and J. W. Hepburn, J. Chem. Phys. **88**, 6658 (1988).
[22] J. P. Holland and R. N. Rosenfeld, J. Chem. Phys. **89**, 7217 (1988).
[23] B. Venkataraman, H. Hou, Z. Zhang, S. Chen, G. Bandukwalla, and M. Vernon, J. Chem. Phys. **92**, 5338 (1990).
[24] D. J. Bogan and D. W. Setser, J. Chem. Phys. **64**, 586 (1976).
[25] J. L. Kinsey, J. Chem. Phys. **54**, 1206 (1971).
[26] In evaluating a similar expression for the distribution in their diatomic product Bogan and Setser[24] replaced the sum over J by an integral. In this approximation the squared term in $(E - E_l - E_v)$ disappears.
[27] M. Bernstein, J. D. Simon, and K. S. Peters, Chem. Phys. Lett. **100**, 241 (1983).
[28] H. Hippler and J. Troe, in *Bimolecular Collisions*, edited by M. N. R. Ashfold and J. E. Baggott (Advances in Gas-Phase Photochemistry and Kinetics, Royal Society of Chemistry, London, 1989).
[29] L. A. Barnes and C. W. Bauschlicher, Jr., J. Chem. Phys. **91**, 314 (1989).
[30] L. A. Barnes, M. Rosi, and C. W. Bauschlicher, Jr., J. Chem. Phys. **93**, 609 (1990).
[31] M. R. A. Blomberg, U. B. Brandemark, P. E. M. Siegbahn, J. Wennerberg, and C. W. Bauschlicher, Jr., J. Am. Chem. Soc. **110**, 6650 (1988).
[32] J. K. Burdett, J. Chem. Soc. Faraday Trans. **70**, 1599 (1974).
[33] M. Elian and R. Hoffman, Inorg. Chem. **14**, 1058 (1975).
[34] T. Beyer and D. F. Swinehart, Commun. Assoc. Comput. Machin. **16**, 379 (1973).
[35] S. E. Stein and B. S. Rabinovitch, J. Chem. Phys. **58**, 2438 (1973).
[36] L. H. Jones, R. S. McDowell, and M. Goldblatt, Inorg. Chem. **8**, 2349 (1969).